UNCLASSIFIED

AD 445239

DEFENSE DOCUMENTATION CENTER

FOR

SCIENTIFIC AND TECHNICAL INFORMATION

CAMERON STATION, ALEXANDRIA, VIRGINIA

UNCLASSIFIED

NOTICE: When government or other drawings, specifications or other data are used for any purpose other than in connection with a definitely related government procurement operation, the U. S. Government thereby incurs no responsibility, nor any obligation whatsoever; and the fact that the Government may have formulated, furnished, or in any way supplied the said drawings, specifications, or other data is not to be regarded by implication or otherwise as in any manner licensing the holder or any other person or corporation, or conveying any rights or permission to manufacture, use or sell any patented invention that may in any way be related thereto.

CATALOGED BY DDC
AS AD 445239

A NEW THERMAL NEUTRON FLUX DENSITY STANDARD*

C. K. HARGROVE AND K. W. GEIGER
Division of Applied Physics, National Research Council, Ottawa, Canada
Received January 30, 1964

ABSTRACT

Six Am^{241}–Be(α, n) neutron sources are arranged around the central circumference of a graphite cylinder 28 cm in diameter by 26.5 cm high. This assembly is surrounded by 10 cm of polyethylene. The graphite cylinder contains an accessible central cavity, 5 cm in diameter by 5 cm high, for the calibration of thermal neutron detectors. The thermal neutron flux density in the cavity is measured by $4\pi\beta$–γ coincidence counting of irradiated gold foils. A flux density below cadmium cutoff of $n_{th}v_0 = 8.70 \times 10^3$ cm^{-2} sec^{-1} ($\pm 1.5\%$) was found. The uniformity is shown to be constant within the cavity to better than $\pm 0.5\%$ over a cylindrical volume 5 cm in diameter by 2 cm high.

1. INTRODUCTION

The accurate determination of thermal neutron flux densities for reactor application or for calibration of neutron detecting equipment has become increasingly important. To meet this need several laboratories (De Juren and Rosenwasser 1954; Axton 1963*a*; Mateescu and Nahorniak 1962; Michikawa *et al.* 1961) have constructed systems which produce a constant and accurately known flux density of thermal neutrons. Three of these use some fixed geometrical arrangement of neutron sources and moderators, although Axton (1963*a*) has made use of a reactor running at low power as a temporary standard. These standard sources of thermal neutrons are used to calibrate detectors. The construction and absolute calibration of the standard thermal neutron flux density at the National Research Council of Canada is described in this paper.

2. CONSTRUCTION OF THE STANDARD

A diagram of the geometry is shown in Fig. 1. The main body, a cylinder 26.5 cm high by 28 cm in diameter, is made of reactor grade graphite. The density was 1.63 g/cm^3 and the manufacturer quoted a thermal neutron absorption cross section of 4.4 millibarns. A removable central cylinder allows access to the irradiation area, a cavity 5 cm high by 5 cm in diameter. Detector foils can be supported in the center of the cavity on cellulose tape, and an axial hole allows counter leads to be taken out if necessary. Six Am^{241}–Be(α, n) sources are embedded around the circumference of the main graphite body at 60° intervals, alternately 1.27 cm above and below the center line. The entire assembly is surrounded with 10 cm of polyethylene. Aluminum tubes are incorporated where necessary to provide proper alignment and stability.

The irradiation of the neutron detectors in an air cavity and in a material having a long mean free path for thermal neutrons simplifies flux density measurements in that the correction for flux depression becomes negligible. This can be explained by considering that the farther from a detector that a

*Issued as N.R.C. No. 8010.

DDC
RECEIVED
AUG 28 1964
DDC-IRA D

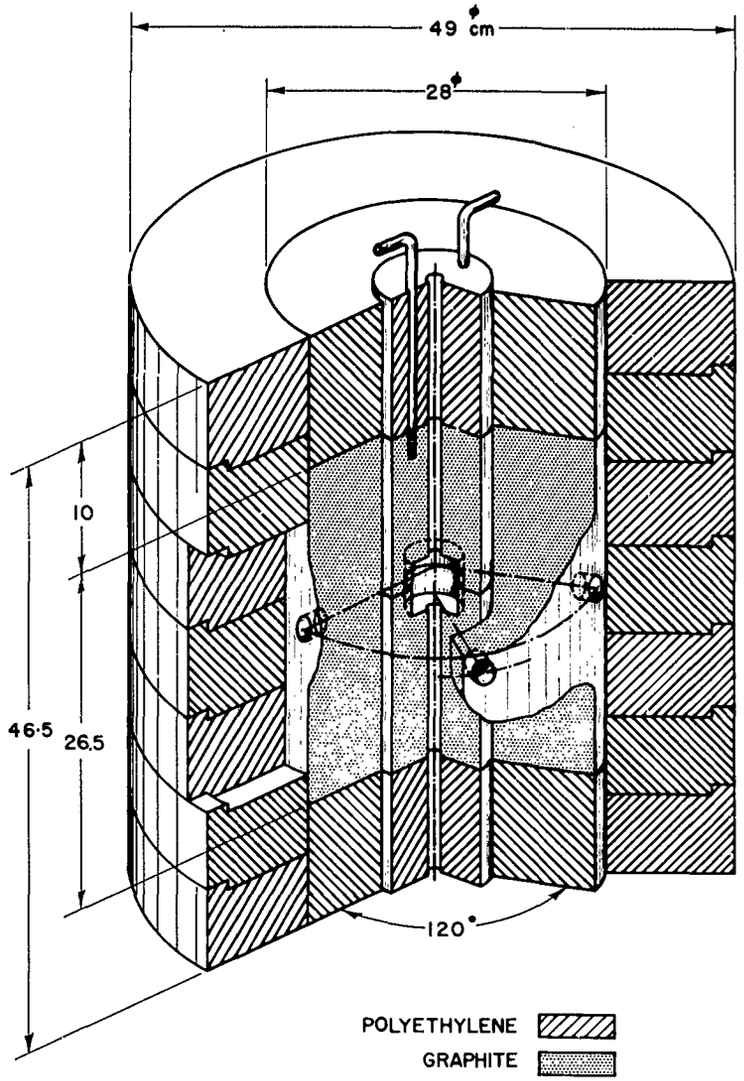

FIG. 1. Thermal neutron flux geometry.

neutron undergoes its first scattering after passing through the detector, the smaller is its chance of being scattered back into the foil. Since the neutrons will undergo many scatterings and be only slightly absorbed, the flux at the irradiation area should be very isotropic.

Good reflection and thermalization are provided by the polyethylene surrounding the graphite. Thermal neutrons leaving the graphite have a high probability, about 0.8, of being reflected back into the graphite by the polyethylene (Wortman 1958). It might be thought that surrounding the central graphite cylinder with a graphite reflector would give a system with a higher flux density since it would absorb fewer neutrons. However, since such a graphite reflector thermalizes the fast source neutrons much farther from the irradiation area than the polyethylene, the chance of the neutrons diffusing back to the center is greatly reduced. Further, the high reflectivity of the poly-

ethylene for thermal neutrons in the central graphite cylinder would be lost. Polyethylene instead of the usual paraffin guarantees long-term mechanical stability.

The recent availability of americium-241 has allowed its use in the fabrication of alloyed Am–Be sources (Runnalls and Boucher 1956). These are used in preference to the more common radium–beryllium sources for the following reasons:

1. A much lower gamma background is produced, hence reducing the shielding requirements.
2. Only a simple decay correction with a half-life of 458 years needs to be applied, compared with radium where the growth of Pb^{210} with a 20-year half-life needs to be considered.
3. Since it is possible to produce an alloyed source, it should be physically stable.

The neutron emission of each of the six sources was compared with the N.R.C. neutron standard (Geiger 1960). A total of 9.45×10^6 neutrons sec^{-1} are emitted by the six sources used in the construction of the flux. The neutron spectrum of one of the sources was also measured (Geiger and Hargrove 1964) and found to be similar to that of other Be(α, n) sources.

3. THE FLUX DENSITY MEASUREMENT

(a) Theory

The neutron flux density is deduced from the reaction rate in detector foils. For a foil, thin enough not to alter the neutron flux, the reaction rate per gram is

$$R = N \int_0^\infty \sigma(v) n(v) v \, dv, \tag{1}$$

where N is the number of atoms per gram in the foil,
$n(v)$ is the neutron density per unit velocity interval,
v is the neutron velocity, and
σ is the reaction cross section.

For a cross section which is proportional to $1/v$ one obtains

$$\sigma(v) = \sigma_0 v_0 / v \quad \text{and} \quad R = N\sigma_0 v_0 \int_0^\infty n(v) dv = N\sigma_0 n v_0. \tag{2}$$

The integral now represents the neutron density n, which is independent of energy. σ_0 is the reaction cross section at $v_0 = 2200$ m/sec and nv_0 is known as the "conventional" flux density which is stated for a velocity of 2200 m/sec. This is in contrast to the "true" average flux $n\bar{v}$ which requires a knowledge of the neutron spectrum or of the neutron temperature in the case of a Maxwellian spectrum.

For most detector substances the cross section departs from a $1/v$ law, particularly in the nonthermal region. It is therefore convenient to use the cadmium difference method and to limit the integral in equation (2) at v_{Cd}, corresponding to the Cd cutoff energy. Then

$$R - R_{Cd} = N\sigma_0 n_{th} v_0,$$

where R_{Cd} is the reaction rate in the detector foil under cadmium and $n_{th}v_0$ is the thermal flux density below cadmium cutoff. Thus, non-Maxwellian flux characteristics become relatively unimportant and different flux assemblies are comparable. After applying all significant corrections, the thermal neutron flux density becomes

$$n_{th}v_0 = \frac{R - R_{Cd}F_{Cd}}{G(t)Ng\sigma_0}, \tag{3}$$

where R is the reaction rate per gram (R_{Cd} with cadmium cover),

F_{Cd} is a correction factor for the absorption of epithermal neutrons by the cadmium cover,

$G(t)$ takes account of the finite thickness, t, of the foil (self-shielding, edge effect, and flux depression),

g takes account of a departure of the cross section from a $1/v$ law within the thermal region; $g = 1$ for a pure $1/v$ absorber (Westcott *et al.* 1958).

The values for $G(t)$ and g depend on the neutron temperature, which is assumed to be 20° C.

It is felt that the flux density in this type of assembly is described best by equation (3). The Westcott convention which is used for the measurement of reactor fluxes gives the total flux density nv_0; however, the Westcott convention uses parameters which have been evaluated for an epithermal flux density with an intensity varying proportional to $1/E$. Calculation of the neutron spectrum in the present geometry (Fowler and Hargrove 1963) shows that it does not vary as $1/E$ because of leakage, and therefore the Westcott convention is not applied. Until the spectrum of epithermal neutrons is measured, it was felt unwise to give an estimate of the total flux density nv_0.

(b) Gold as a Detector

The thermal neutron flux density was measured by activation of gold foils. Gold was used for the following reasons:

1. It is a monoisotopic element and can be obtained in high purity.

2. Its thermal neutron cross section is one of the best known and large enough to give sufficient activation. The generally accepted value, $\sigma_0 = 98.8 \pm 0.3$ barns (Hughes and Schwartz 1958), has been used.

3. The disintegration scheme of Au^{198} allows the determination of the absolute activity by coincidence counting, thereby eliminating the need of a correction for β-counting efficiency.

4. The deviation from a $1/v$ cross section below cadmium cutoff is small, resulting in a Westcott g factor of only 1.0053 (Westcott 1960).

5. The half-life of Au^{198}, equal to 2.696 days, is short enough to allow reasonable irradiation times.

(c) Corrections for Flux Depression, Self-Shielding, and Edge Effect

The flux depression in graphite for gold foils (0.001 in. thick and 10 mm in diameter) as used in the present experiment, is 0.2% (Bothe 1943; Tittle 1951). However, the foils are irradiated in an air cavity which reduces this flux

depression considerably (see Section 2). The edge effect, which increases activation, is 0.15% for a 0.001-in. foil (Hanna 1963). These effects will tend to cancel each other and have been neglected. The $G(t)$ correction therefore accounts for the self-shielding in the detector material only and is (Bothe 1943)

$$G(t) = \frac{1}{t\Sigma_{eff}} \left(\tfrac{1}{2} - E_3(t\Sigma_{eff})\right),$$

where t is the thickness of the foil,

Σ_{eff} is the macroscopic effective absorption cross section, and

$E_3(x)$ is the third-order exponential integral.

The effective cross section for the self-shielding correction must take into account that the self-shielding is different for the different neutron velocities. Mosburg (1961) has shown that for foils with $t\Sigma \leq 0.09$ a value of $\Sigma_{eff} = 1.08\ \Sigma_0$ gives a sufficiently good approximation to the exact solution. The calculated values for the self-shielding are given in Table II.

(d) Attenuation of Epithermal Neutrons by the Cadmium Cover

The factor F_{Cd} takes into account the attenuation of the epithermal flux by the cadmium cover, which results in too low a gold-foil activation under cadmium. The attenuation can be calculated; in sufficient approximation it is (Tittle 1951)

$$1/F_{Cd} = 2\ E_3(\delta\Sigma_{Cd}),$$

where δ is the cadmium thickness and Σ_{Cd} is the macroscopic cadmium cross section at the gold resonance energy. A value of $F_{Cd} = 1.048$ for a 1-mm cover follows when using the total cadmium cross section of 5.3 barns. However, this value of F_{Cd} is believed to be too high, since attenuation in this geometry is predominantly determined by the cadmium absorption cross section, which is not known at the gold resonance energy.

It seems more desirable to use an experimental determination of F_{Cd} by making epithermal neutron activation measurements with various cadmium thicknesses and extrapolating to zero thickness. In first approximation this yields F_{Cd} directly. Measurements were carried out with 1-mm and 2-mm cadmium covers; this resulted in a value of $F_{Cd} = 1.01 \pm 0.01$ for the 1-mm cover used in the measurements. Two published values for gold foil under cadmium cover, activated in graphite, are available: $F_{Cd} = 1.01$ (Axton 1963*a*) and $F_{Cd} = 1.02$ (Martin 1955). The factor F_{Cd} is not needed with great accuracy since its effect on the final result, $n_{th}v_0$, is small. A value of $F_{Cd} = 1.01$ has been adopted.

4. ABSOLUTE COUNTING OF GOLD FOILS

The reaction rate of the neutrons in the gold foil is found by measuring the absolute activity of the gold foils by $4\pi\beta$–γ coincidence counting; apparatus and method have been described by Campion (1959). The equipment differed only in that the γ detectors were two NaI(Tl) crystals 2 in. × 2 in. in size. The advantage of the $4\pi\beta$–γ coincidence method lies in the fact that, because of high β-detection efficiency in the $4\pi\beta$ counter, most corrections are small.

High β efficiency may not necessarily be achieved with foils, but the corrections described by Campion (1959) may be used to extend the method to lower efficiencies (Axton 1963*a*). A window in the γ channel was set to include only the 412-keV photopeak of Au^{198} so as to minimize the γ background. Since all rates were low, dead-time losses and accidental coincidences could be neglected.

The disintegration rate n_0 for a gold foil may be represented by

$$n_0(1 + K_1)(1 + K_2) = n_\beta n_\gamma / n_c, \tag{4}$$

where n_β, n_γ, and n_c are the count rates in the γ, β, and coincidence channels, corrected for background. K_1 is a correction for the complex decay scheme and K_2 a correction for internal conversion and γ sensitivity of the $4\pi\beta$ counter. Both are negligible for β efficiencies close to 100%.

(a) The Decay Scheme Correction, K_1

Without correction the $4\pi\beta$–γ coincidence method is only valid for cases where a single β branch is followed by one or more γ transitions. The disintegration scheme of Au^{198} (Fig. 2) has two additional weak β transitions, and

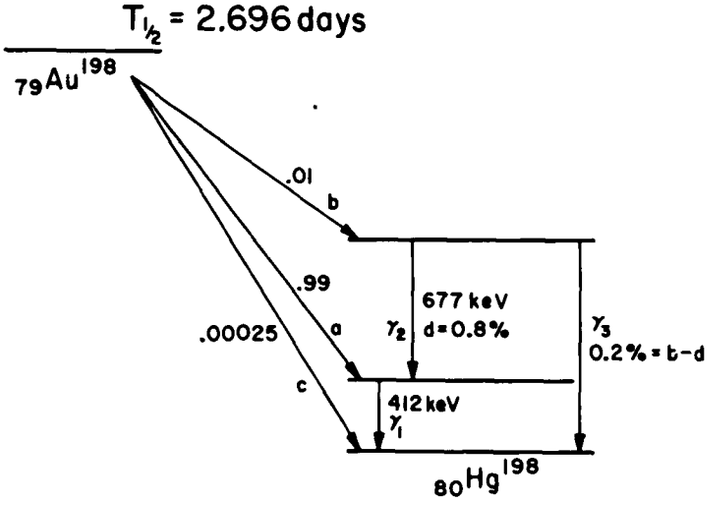

FIG. 2. The decay scheme of Au^{198}.

a decay scheme correction K_1 has to be applied. Neglecting very small contributions from the β transition into the ground state, the counting rates for the individual channels are as follows:

$$n_\beta = n_0(a\epsilon_{\beta a} + b\epsilon_{\beta b}), \qquad n_\gamma = n_0\left[\frac{a+d}{1+\alpha}\epsilon_{\gamma 1} + d\epsilon_{\gamma 2} + (b-d)\epsilon_{\gamma 3}\right],$$

$$n_c = n_0\left[\frac{a\epsilon_{\gamma 1}}{1+\alpha}\epsilon_{\beta a} + \left(\frac{d\epsilon_{\gamma 1}}{1+\alpha} + d\epsilon_{\gamma 2} + (b-d)\epsilon_{\gamma 3}\right)\epsilon_{\beta b}\right],$$

and therefore

$$\frac{n_\beta n_\gamma}{n_c} = n_0(1 + K_1)$$

with $$K_1 = \frac{(f-b)(1-\epsilon_{\beta b}/\epsilon_{\beta a})}{1+f\epsilon_{\beta b}/a\epsilon_{\beta a}},$$

where $$f = d\left(1+\frac{\epsilon_{\gamma 2}(1+\alpha)}{\epsilon_{\gamma 1}}-\frac{\epsilon_{\gamma 3}(1+\alpha)}{\epsilon_{\gamma 1}}\right)+b\frac{\epsilon_{\gamma 3}(1+\alpha)}{\epsilon_{\gamma 1}}.$$

The small letters are the β-transition probabilities in the disintegration scheme of Au^{198} as shown in Fig. 2, and the efficiencies ϵ refer to the respective branches as indicated in the figure. The coefficient α is the conversion coefficient for the 412-keV γ transition, γ_1, of 0.043.

For the appropriate values of the efficiencies, $\epsilon_{\gamma 2}/\epsilon_{\gamma 1} = 0.2$, and $\epsilon_{\gamma 3}/\epsilon_{\gamma 1} = 0.1$, estimated from the γ-window setting and counting efficiencies (Heath 1957), K_1 is less than 0.001 for any possible combination of β efficiencies and for any of the foils used in the experiment.

(b) Correction for Internal Conversion and for Gamma Efficiency of the Beta Counter, K_2

In calculating these corrections the approximation is made that there is only the main β branch involved, followed by the 412-keV transition to the ground state. Then the counting rates for the individual channels are

$$n_\beta = n_0\epsilon_\beta\left[1+\frac{1-\epsilon_\beta}{\epsilon_\beta(1+\alpha)}(\alpha\epsilon_c+\epsilon_{\beta\gamma})\right], \qquad n_\gamma = \frac{n_0\epsilon_\gamma}{1+\alpha},$$

$$n_c = \frac{n_0\epsilon_\beta\epsilon_\gamma}{1+\alpha}\left(1+\frac{1-\epsilon_\beta}{\epsilon_\beta}\epsilon_{\beta\gamma}\frac{\epsilon_\gamma'}{\epsilon_\gamma}\right),$$

and therefore

$$(5) \qquad \frac{n_\beta n_\gamma}{n_c} \approx n_0\left[1+\frac{1-\epsilon_\beta}{\epsilon_\beta}\left(\frac{\alpha\epsilon_c+\epsilon_{\beta\gamma}}{1+\alpha}-\epsilon_{\beta\gamma}\frac{\epsilon_\gamma'}{\epsilon_\gamma}\right)\right] = n_0(1+K_2);$$

it also follows that

$$(6) \qquad \epsilon_\beta = \left(\frac{n_c}{n_\gamma}-\epsilon_{\beta\gamma}\frac{\epsilon_\gamma'}{\epsilon_\gamma}\right)\Big/\left(1-\epsilon_{\beta\gamma}\frac{\epsilon_\gamma'}{\epsilon_\gamma}\right),$$

where ϵ_c is the efficiency of the β detector for detecting conversion electrons from the 412-keV γ transition,

$\epsilon_{\beta\gamma}$ is the efficiency of the γ detector for detecting γ rays,

ϵ_γ' is the efficiency of the γ detector for γ quanta which emerge from the β detector after interacting in this detector,

α is the conversion coefficient for the 412-keV γ line of 0.043.

In order to calculate K_2, it is necessary to evaluate ϵ_c, $\epsilon_{\beta\gamma}$, and ϵ_γ'. For the conversion electron efficiency, ϵ_c, it might be assumed that all electrons which reach the surface of the gold foil are being counted. Very little information is available on the absorption and scattering of monoenergetic electrons in heavy elements. An upper limit for the conversion electron efficiency was calculated on the assumption that all electrons had their maximum path length (Nelms 1956) and underwent no scattering. A lower limit was calculated on the assumption of no scattering, but electron attenuation following the curve shape as

given by Marshall and Ward (1937). The effect of electron scattering will bring the efficiency somewhere between these two estimates. For the geometrical escape probabilities, see Taylor (1961). The minimum and maximum efficiencies ϵ_c, so obtained are given in Table I for various gold thicknesses t.

TABLE I

Detection probabilities for evaluation of K_2

t (mg/cm²)	ϵ_c (min.)	ϵ_c (max.)	$\epsilon_{\beta\gamma}$	$\epsilon_\gamma'/\epsilon_\gamma$
6	0.96	0.99	0.002	0.15
31	0.83	0.93	0.006	0.12
49	0.75	0.89	0.008	0.09
110	0.48	0.74	0.011	0.09

The γ efficiency of the β counter $\epsilon_{\beta\gamma}$ can be obtained by using the method for calculating the γ efficiency of a Geiger–Müller counter (e.g. Price 1958). However, since with an internal radioactive source the γ radiation penetrates the wall only once, the efficiency is expected to be reduced by a factor of 2. It follows that $\epsilon_{\beta\gamma}$ (wall) = 0.001. The efficiency due to the counting gas is lower by a factor of 10. Of major importance, however, is the contribution of the gold foil itself, from which a considerable number of photoelectrons and Compton electrons are being ejected, depending on the gold thickness. Separate estimates are made for the total efficiency, $\epsilon_{\beta\gamma}$ (foil), of the counter and the efficiency $\epsilon_{\beta\gamma}'$ where the photo efficiency is subtracted. For the calculation, the efficiency for counting the photoelectrons was assumed to be equal to ϵ_c, calculated above.

The efficiency ϵ_γ' will be proportional to ϵ_γ. The proportionality factor will contain $\epsilon_{\beta\gamma}'/\epsilon_{\beta\gamma}$, where $\epsilon_{\beta\gamma}'$, just calculated above, is the probability for γ interactions in the β counter where the γ quanta are not lost by photoeffect. The detection of these remaining Compton-scattered photons depends on whether their energies fall within the γ window. A probability of 0.25 was estimated for the particular window setting used, so that one obtains

$$\epsilon_\gamma' = \epsilon_\gamma \frac{\epsilon_{\beta\gamma}'}{\epsilon_{\beta\gamma}} \times 0.25.$$

Individual values for ϵ_c, $\epsilon_{\beta\gamma}$, and $\epsilon_\gamma'/\epsilon_\gamma$ are given in Table I. The minimum and maximum values of K_2 as a function of n_c/n_γ are shown in Fig. 3. For the activity calculations, the median value has been adopted.

5. RESULTS

(a) Uniformity of Flux Density

To investigate the uniformity of the flux density in the irradiation area, flux mapping was carried out with a manganese foil. Only relative measurements are required and the Mn-foil activity was simply determined in a $4\pi\beta$ counter. The foil was irradiated at the center of the cavity, the outer edge, one centimeter axially down, and at the center with the axis of the foil at 90° to the axis of the flux. The individual irradiations resulted in relative flux

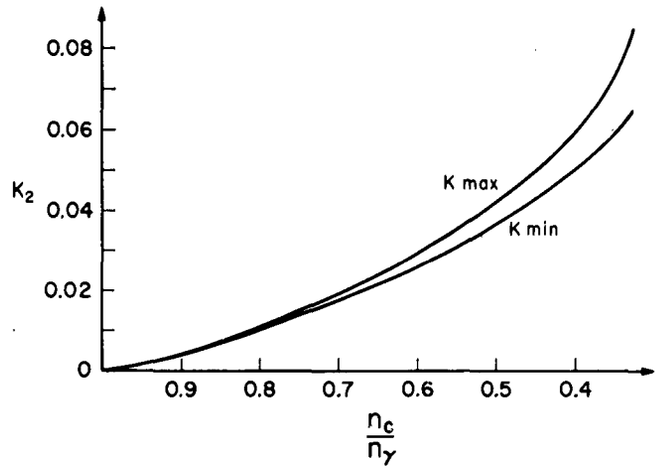

FIG. 3. The correction K_2 for internal conversion of the 412-keV γ line and for the γ sensitivity of the β counter as a function of the measured value n_c/n_γ.

density measurements having a standard deviation of $\pm 0.28\%$. Of the six activations made, two were greater than one stadard deviation from the mean and these were less than 0.33%. The uniformity of the flux density, therefore, is constant to better than $\pm 0.5\%$ over the central irradiation area of 5 cm diameter and 2 cm height.

(b) Flux Density Measurement

Gold foils of nominally 0.1, 0.5, 1.0, and 2 mil thickness and a diameter of 10 mm were irradiated in the center of the cavity. Up to four foils, spaced laterally, were irradiated simultaneously; this arrangement caused no flux depression, as shown when irradiating an additional manganese foil, centered between the gold foils. The manganese activity was the same as obtained in (*a*). All gold goils were irradiated for approximately one week and counted over a period of three days, alternating with background runs. Separate irradiations were carried out with the same foils under 1-mm cadmium cover.

The disintegration rate was evaluated using equation (4) and corrected to give the rate per milligram at saturation. An expression for the fractional standard deviation of the disintegration rate measured by the coincidence technique has been given by Campion and Taylor (1961). However, this expression neglects background rates. For the present measurements, the effect of the background in the γ channel is not negligible, but the error in the background rate itself can be neglected. Then the expression for the fractional deviation in n_0 for a counting period becomes

$$\rho = \left[\frac{1}{N_c}\left(2\epsilon_\beta\epsilon_\gamma - \epsilon_\beta - \epsilon_\gamma + 1 + \epsilon_\beta\frac{b_\gamma}{n_\gamma}\right)\right]^{\frac{1}{2}},$$

where N_c is the number of coincidences during this counting period and b_γ/n_γ the average fractional background rate for this period in the γ channel.

The weighted averages of the reaction rates, together with the combined statistical errors, are shown in Table II. The flux densities are obtained from equation (3). The measured ratios n_c/n_γ are also given; they are very close to

TABLE II

Gold foil activations

t (mg cm^{-2})	$\frac{1}{G(t)}$	n_c/n_γ (%)	R (sec^{-1} mg^{-1})	n_c/n_γ in Cd (%)	R_{Cd} (sec^{-1} mg^{-1})	$n_{th}v_0$ (cm^{-2} sec^{-1})	$(n_{th}v_0)_{av}$ (cm^{-2} sec^{-1})
30.87	1.0287	66.8	3.061±0.012	67	0.496±0.008	8671	
31.03	1.0291	67.1	3.054	69	0.478	8712	8.70×10^3
45.26	1.0397	57.8	2.971±0.011	60	0.414±0.005	8738	
47.13	1.0410	57.4	2.941	59	0.412	8657	
47.29	1.0410	57.1	2.957	60	0.409	8718	
45.28	1.0397	58.4	2.960	60	0.415	8696	

the efficiency of the β counter, ϵ_β (see eq. 6). The measurements for the 0.1- and 2.0-mil foils were not used, because of the larger error involved.

Table III shows how standard deviations and estimated systematic errors for the individual parameters of equation (3) contribute to the final result. The largest contribution is in the systematic error for the gold standardization, where the uncertainties for the conversion coefficient α and for the detection efficiency ϵ_c are the main contributing factors. The resulting uncertainty for the final result then becomes $\pm 1.5\%$.

TABLE III

Contributions to error in final result

	Relative standard deviation (%)		Systematic error (%)
Gold standardization R	0.2	}	0.4
Gold standardization R_{Cd}	0.2	}	
Weight determinations	0.2		
Effective gold cross section $g\sigma$			0.3
Absorption by Cd-cover F_{Cd}			0.2
Self-shielding $G(t)$			0.2
	0.4		1.1
Error in final result		1.5	

6. CONCLUSION

The neutron flux density standard constructed at the National Research Council of Canada has a thermal flux density of

$$n_{th}v_0 = (8.70 \pm 0.13) \times 10^3 \text{ neutrons cm}^{-2} \text{ sec}^{-1}$$

below the cadmium cutoff energy ($v_0 = 2200$ m/sec). It is uniform to $\pm 0.5\%$ over a cylindrical volume 5 cm in diameter by 2 cm high. The standard serves for the calibration of foils and other neutron detectors. The neutrons are produced by Am^{241}–Be sources; because of low γ emission, these sources allowed the construction of a very compact assembly which, through the use of polyethylene instead of paraffin as reflector, should remain stable with time.

ACKNOWLEDGMENTS

The contribution of Dr. Margaret D. Wilson by programming the computer to process the counting data is gratefully acknowledged. The authors also wish to thank Dr. O. J. C. Runnalls, Atomic Energy of Canada Ltd., Chalk River, for the preparation of the neutron source material.

REFERENCES

AXTON, E. J. 1963*a*. Reactor Sci. Techn. **17**, 125.
——— 1963*b*. J. Res. Nat. Bur. Std. **A67**, 215.
BOTHE, E. 1943. Z. Physik, **120**, 437.
CAMPION, P. J. 1959. Intern. J. Appl. Radiation Isotopes, **4**, 232.
CAMPION, P. J. and TAYLOR, J. G. V. 1961. Intern. J. Appl. Radiation Isotopes, **10**, 131.
DE JUREN, J. and ROSENWASSER, H. 1954. J. Res. Nat. Bur. Std. **52**, 93.

FOWLER, A. G. and HARGROVE, C. K. 1963. Unpublished.
GEIGER, K. W. 1960. Can. J. Phys. **38**, 569.
GEIGER, K. W. and HARGROVE, C. K. 1964. Nucl. Phys. **53**, 204.
HANNA, G. C. 1963. Nucl. Sci. Eng. **15**, 325.
HEATH, R. L. 1957. U. S. At. Energy Comm. Report IDO-16408.
HUGHES, D. J. and SCHWARTZ, R. B. 1958. U.S. At. Energy Comm. Report B.N.L. 325, 2nd ed.
MARSHALL, J. S. and WARD, A. G. 1937. Can. J. Res. **A15**, 39.
MARTIN, D. H. 1955. Nucleonics, **13** (3), 52.
MATEESCU, N. and NAHORNIAK, V. 1962. Stud. Cerc. Fiz. Acad. R.P.R. **13**, 375.
MOSBURG, E. R. 1961. Unpublished. As quoted by Axton (1963*a*).
MOSBURG, E. R. and MURPHEY, W. M. 1961. Reactor Sci. Technol. **14**, 25.
MICHIKAWA, T., FURUBAYASHI, B., TERANISHI, E., and INOUE, Y. 1961. Bull. Electrotech. Lab. (Tokyo), **25**, 843.
NELMS, A. J. 1956. Natl. Bur. Std. (U.S.), Circ. 577.
PRICE, W. J. 1958. Nuclear radiation detection (McGraw-Hill Book Company).
RUNNALS, O. J. C. and BOUCHER, R. R. 1956. Can. J. Phys. **34**, 959.
TAYLOR, J. G. V. 1961. Unpublished. As quoted by Axton (1963*a*).
TITTLE, C. W. 1951. Nucleonics, **9** (1), 60.
WESTCOTT, C. H. 1960. At. Energy Can. Ltd. Report No. 1101.
WESTCOTT, C. H., WALKER, W. H., and ALEXANDER, T. K. 1958. Proc. Second Intern. Conf. Peaceful Uses At. Energy, Geneva, A/Conf. 15/P/202.
WORTMAN, H. 1958. Diplom-Arbeit, Physikalisch-Technische Bundesanstalt, Braunschweig, West Germany.